The EMBO Journal Vol. 21 No. 6 pp. 1289–1300, 2002

Late endosome motility depends on lipids via the small GTPase Rab7

Cécile Lebrand[1], Michela Corti[1], Holly Goodson[2,3], Pierre Cosson[4], Valeria Cavalli[1], Nathalie Mayran[1], Julien Fauré[1] and Jean Gruenberg[1,5]

[1]Department of Biochemistry, University of Geneva, Sciences II, [2]Department of Cell Biology, University of Geneva, Sciences III, 30 quai E.Ansermet and [4]Centre Medical Universitaire, Departement de Morphologie, 1 rue Michel Servet, 1211 Geneva 4, Switzerland

[3]Present address: University of Notre Dame, Department of Chemistry and Biochemistry, 251 Nieuwland Science Hall, Notre Dame, IN 46556-5670, USA

[5]Corresponding author
e-mail: jean.gruenberg@biochem.unige.ch

C.Lebrand and M.Corti contributed equally to this work

We report that lipids contribute to regulate the bidirectional motility of late endocytic compartments. Late endocytic vesicles loaded with cholesterol lose their dynamic properties, and become essentially immobile, including in cells from Niemann–Pick C patients. These vesicles then retain cytoplasmic dynein activity, but seem to be unable to acquire kinesin activity, eventually leading to paralysis. Our data suggest that this defect depends on the small GTPase Rab7, since the motility of vesicles loaded with cholesterol can be restored by the Rab7 inhibitory mutant N125I. Conversely, wild-type Rab7 overexpression mimics the effects of cholesterol on motility in control cells. Consistently, cholesterol accumulation increases the amounts of membrane-associated Rab7, and inhibits Rab7 membrane extraction by the guanine nucleotide dissociation inhibitor. Our observations thus indicate that cholesterol contributes to regulate the Rab7 cycle, and that Rab7 in turn controls the net movement of late endocytic elements. We conclude that motor functions can be regulated by the membrane lipid composition via the Rab7 cycle.

Keywords: cholesterol/cytoplasmic dynein/kinesin/lysobisphosphatidic acid/Niemann–Pick type C

Introduction

After internalization, cell surface proteins, lipids and solutes first appear in peripheral early endosomes. From there, molecules can be recycled back to the cell surface, at least in part via recycling endosomes, or selectively transported to late endosomes and lysosomes for degradation. It has long been known that endosomes move from the periphery towards the pericentriolar region along the degradation pathway, and that this long-distance transport depends on microtubules (Pastan and Willingham, 1981) and the minus-end-directed motor cytoplasmic dynein (Bomsel *et al*., 1990; Schroer and Sheetz, 1991; Aniento *et al*., 1993; Oda *et al*., 1995; Harada *et al*., 1998; Wubbolts *et al*., 1999). It has also become apparent that late endosomes and lysosomes exhibit bidirectional motility, and then use plus-end-directed kinesins when moving towards the cell periphery (Hollenbeck and Swanson, 1990; Feiguin *et al*., 1994; Rodriguez *et al*., 1996; Santama *et al*., 1998; Tanaka *et al*., 1998; Wubbolts *et al*., 1999). Bidirectional motility presumably ensures that the dynamic properties of these membranes are maintained, but the mechanisms that regulate motor activity are not known.

Recent studies reveal that some lipids are not randomly distributed within endosomal membranes, and that these lipids are involved directly in protein sorting and membrane transport (Gruenberg, 2001). In particular, the raft lipids cholesterol and sphingomyelin may play a role in protein sorting along the recycling circuit (Mayor *et al*., 1998). Phosphoinositol-3-phosphate (PI3P) is found predominantly at early stages of the endocytic pathway (Gillooly *et al*., 2000), and interacts specifically with numerous proteins that regulate transport (Simonsen and Stenmark, 2001; Simonsen *et al*., 2001). Finally, at the next step of the pathway, membrane invaginations within late endosomes contain high amounts of the unusual phospholipid lysobisphosphatidic acid (LBPA), which is involved in cholesterol transport and protein trafficking (Kobayashi *et al*., 1998b, 1999). In this study, we provide evidence that the motility of late endocytic compartments depends on the membrane lipid composition via the small GTPase Rab7.

Results

Dynamics of late endocytic compartments containing CD63–GFP

CD63/Lamp3 can be detected at the cell surface, at least in some cell types, but is present mostly in late endocytic compartments, like Lamp1 and Lamp2 (Kornfeld and Mellman, 1989; Fukuda, 1991; Metzelaar *et al*., 1991; Escola *et al*., 1998; Kobayashi *et al*., 1999). Here, we used wild-type CD63/Lamp3 tagged at the cytoplasmically oriented N-terminus with green fluorescent protein (CD63–GFP) to study the dynamic properties of late endocytic compartments by video microscopy. CD63–GFP was expressed properly in BHK and HeLa cells, and, like CD63, distributed to late endocytic compartments, where it co-localized with the late endosomal lipid LBPA, and with Lamp1, Lamp2 and cathepsin D (not shown). Time-lapse video microscopy showed that CD63–GFP (Figure 1A) or Lamp1–GFP (not shown) was present within vesicles and abundant tubules, and that both exhibited linear, bi-directional, saltatory motion between the periphery and the perinuclear region. In this and all subsequent sequences, images were collected at 1 s

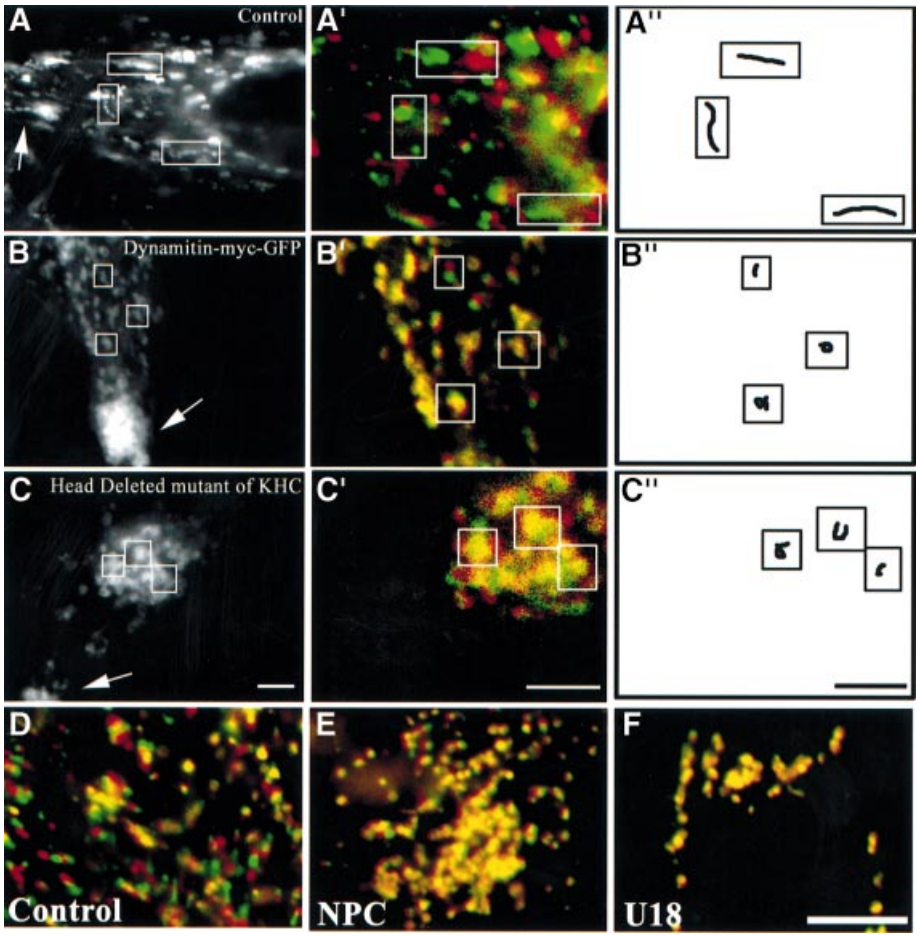

Fig. 1. Motility and cholesterol accumulation. (A–C) HeLa cells were transfected with CD63–GFP (**A**) or co-transfected with CD63–GFP and either dynamitin-myc–GFP (**B**), or a head-deleted mutant of KHC (**C**). Dynamitin-myc–GFP remained exclusively cytosolic, and was not detected after 100–200 ms exposure times; co-expression was verified by indirect immunofluorescence using anti-myc antibodies for dynamitin, or the Suk4 anti-kinesin antibody for the KHC mutant (endogenous and overexpressed KHC were easily distinguished by the intensity of the signal). Images were collected at 1 s interval over a time period of 25 s and then all images were stacked; arrows point to the cell periphery. Then, a moving object appears as a series of closely associated spots that reveals its track, as in the control cell in (A). (**A′–C′**) Initial and final positions were color-coded in red and green, respectively: a moving object is both red and green, and an immobile object yellow. (**A″–C″**) Traces of individual elements. Control (**D** and **F**) or NPC (**E**) fibroblasts were incubated at 37°C for 13 h with Alexa568-labeled antibodies against CD63 without (D and E) or with (F) 3 μg/ml U18666A, and analyzed as above (A′–C′). Bars: (A–C) 2 μm; (D–F) 3.7 μm.

interval over a total time period of 25 s to visualize better the trace of individual elements and limit light damage (except in Figure 2A that shows 5 min sequences with 12 s intervals). Tubules appeared to form by vesicle elongation or by fission, and then moved rapidly in the cytoplasm (0.5 ± 0.2 μm/s), with frequent pauses. They often encountered other tubules or vesicles, with which they fused, as expected (Aniento *et al*., 1993; Mullock *et al*., 1998). CD63–GFP was thus present within highly dynamic tubulo-vesicular networks, which correspond to both late endosomes and lysosomes (referred to here as late endocytic compartments).

Microtubules and motors

The motility of vesicles and tubules containing CD63–GFP was microtubule dependent, as expected (Schroer and Sheetz, 1991). Microtubule depolymerization with nocodazole caused the dispersion of CD63–GFP-positive elements and abolished motility, while depolymerization of actin filaments with cytochalasin D had no effect (not shown). Inactivation of cytoplasmic dynein, caused by dynamitin overexpression (Allan and Schroer, 1999), significantly reduced motility, and CD63–GFP-labeled vesicles accumulated at the cell periphery (Figure 1B), in agreement with previous studies (Vallee and Sheetz, 1996; Valetti *et al*., 1999). Conversely, overexpression of the motor head-deleted mutant of conventional kinesin, HsuKHC/Kif5B (Wubbolts *et al*., 1999), inhibited motility and caused perinuclear vesicle accumulation (Figure 1C), as expected (Feiguin *et al*., 1994; Tanaka *et al*., 1998; Wubbolts *et al*., 1999). Under all these inhibitory conditions, tubules were no longer observed, suggesting that their biogenesis and dynamics depend on microtubules and motors.

NPC cells and cells treated with drugs that mimic NPC

Niemann–Pick type C (NPC) is a storage disorder caused by cholesterol accumulation within late endocytic compartments (Liscum and Klansek, 1998), containing both LBPA and CD63 (Kobayashi *et al*., 1999). Very recent studies reveal that late endocytic movements depend on an

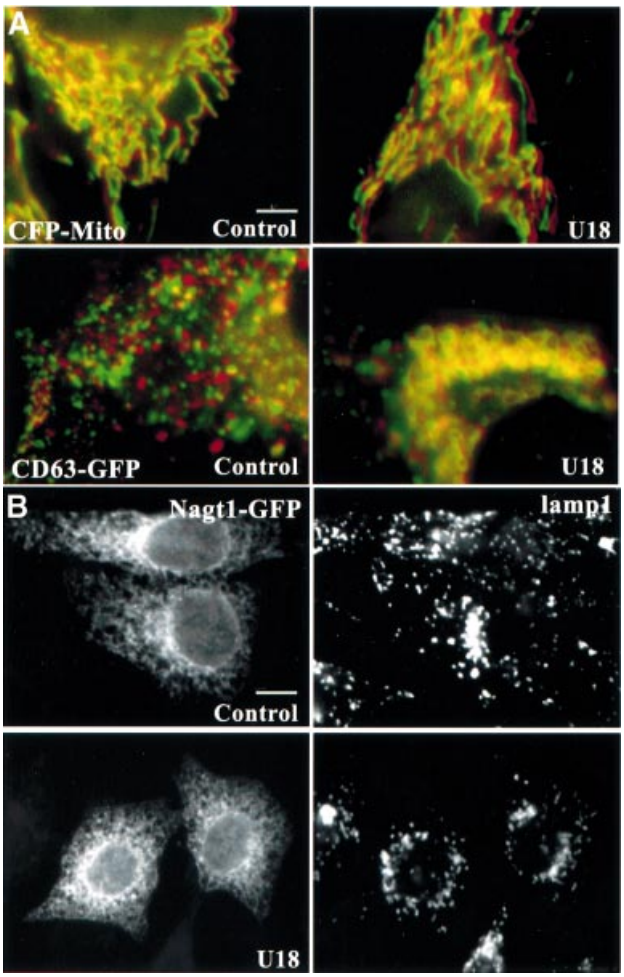

Fig. 2. Other organelles. (**A**) HeLa cells transfected with the mitochondrial marker ECFP (CFP-mito) or with CD63–GFP were treated or not with U18666A. Frames were captured every 12 s to limit light damage, over 5 min to visualize better mitochondrial motility, and analyzed as in Figure 1A′–C′. (**B**) HeLa cells expressing NAGT1–GFP treated or not with U18666A and then with brefeldin A for 30 min, as indicated, were labeled with anti-Lamp1 antibodies and processed for microscopy. Bars: (A) 3.9 μm; (B) 6.2 μm.

intact NPC1 protein (Zhang *et al*., 2001), and that the dynamics of organelles containing mutant NPC1 protein are impaired (Ko *et al*., 2001). When endogenous CD63 of NPC cells was labeled with endocytosed antibodies, CD63-positive elements were abundant and swollen, as expected after cholesterol accumulation (Neufeld, 1991; Kobayashi *et al*., 1999), and their motility was essentially abolished (Figure 1E), when compared with control fibroblasts (Figure 1D). In marked contrast, the motility of late endocytic compartments was not affected in Tay–Sachs fibroblasts (not shown), a sphingolipid storage disorder that is not accompanied by cholesterol accumulation (Chen *et al*., 1999; Kobayashi *et al*., 1999).

Motility could also be inhibited in normal fibroblasts by the hydrophobic amine U18666A (Figure 1F), which causes cholesterol accumulation in late endosomes, like NPC (Liscum and Faust, 1989; Kobayashi *et al*., 1999). We thus used U18666A in HeLa cells expressing CD63–GFP to quantify motility in a non-pathological genetic background (see Figure 5A). After the treatment, ~90% of the labeled vesicles exhibited Brownian-type motion and remained confined within 0.7 μm of their initial position after 25 s, in contrast to 30% in control cells (see Figure 5E). Tubules were rarely observed in NPC cells or drug-treated cells, indicating that tubulo-vesicular networks had mainly collapsed into large, relatively passive vacuoles. In addition, cholesterol accumulation also caused a characteristic accumulation of late endocytic compartments in the perinuclear region (Figure 2A, CD63–GFP; Figure 2B, Lamp1 at low magnification). Motility inhibition was not due to some general or indirect effect of the treatment on microtubules and motors, since neither the distribution nor the motility of mitochondria were affected when the motility of late endocytic compartments was inhibited (even over a long, 5 min time period, Figure 2A). Similarly, cholesterol accumulation did not interfere with the microtubule-dependent redistribution (Lippincott-Schwartz *et al*., 1990) of the Golgi enzyme *N*-acetylglucosamine-transferase 1 (NAGT1)–GFP (Shima *et al*., 1997) to the endoplasmic reticulum in the presence of brefeldin A (Figure 2B).

Lysobisphosphatidic acid

We then made use of the 6C4 monoclonal antibody against the unusual phospholipid LBPA to investigate more directly the possible role of lipids in motility. In previous studies, we showed that LBPA is a major constituent of the lumenal membrane invaginations of multivesicular/multilamellar late endosomes, and is not detected elsewhere in the cell (Kobayashi *et al*., 1998b). When internalized by fluid phase endocytosis, the 6C4 antibody accumulates in late endosomes upon binding to its antigen, and causes cholesterol accumulation within late endosomes, indicating that LBPA-rich internal membranes are involved in cholesterol transport from late endosomes (Kobayashi *et al*., 1999). Much like in NPC or U18666A-treated cells, the endocytosed 6C4 antibody inhibited late endosome motility (Figure 3B), when compared with control cells (Figure 3A). In marked contrast, motility was not affected by endocytosed antibodies against Lamp1 (Figure 3C), which co-localizes with LBPA in late endosomes but is restricted to the limiting membrane (Griffiths *et al*., 1988; Aniento *et al*., 1993; Kobayashi *et al*., 1998b). These experiments show that motility was selectively inhibited, presumably because of cholesterol accumulation, when interfering with LBPA functions in the endosomal lumen.

Motility of cholesterol-laden endosomes is selectively impaired

We further investigated whether cholesterol accumulation interfered selectively with late endocytic compartment dynamics in HeLa cells treated with U18666A, by following an endocytosed pulse of Oregon green-labeled dextran (Figure 3D). After a short chase (15–30 min), labeled endosomes clearly moved in a centripetal fashion, as expected during transport from early to late endosomes (Pastan and Willingham, 1981; Herman and Albertini, 1984). Motility decreased during a subsequent chase, and was essentially abolished after 90–120 min, when the tracer had reached swollen, cholesterol-laden and Lamp1-positive vesicles in the perinuclear region (Figure 3E), in contrast to control cells (not shown, see above). This behavior was not due to some indirect exhaustion of

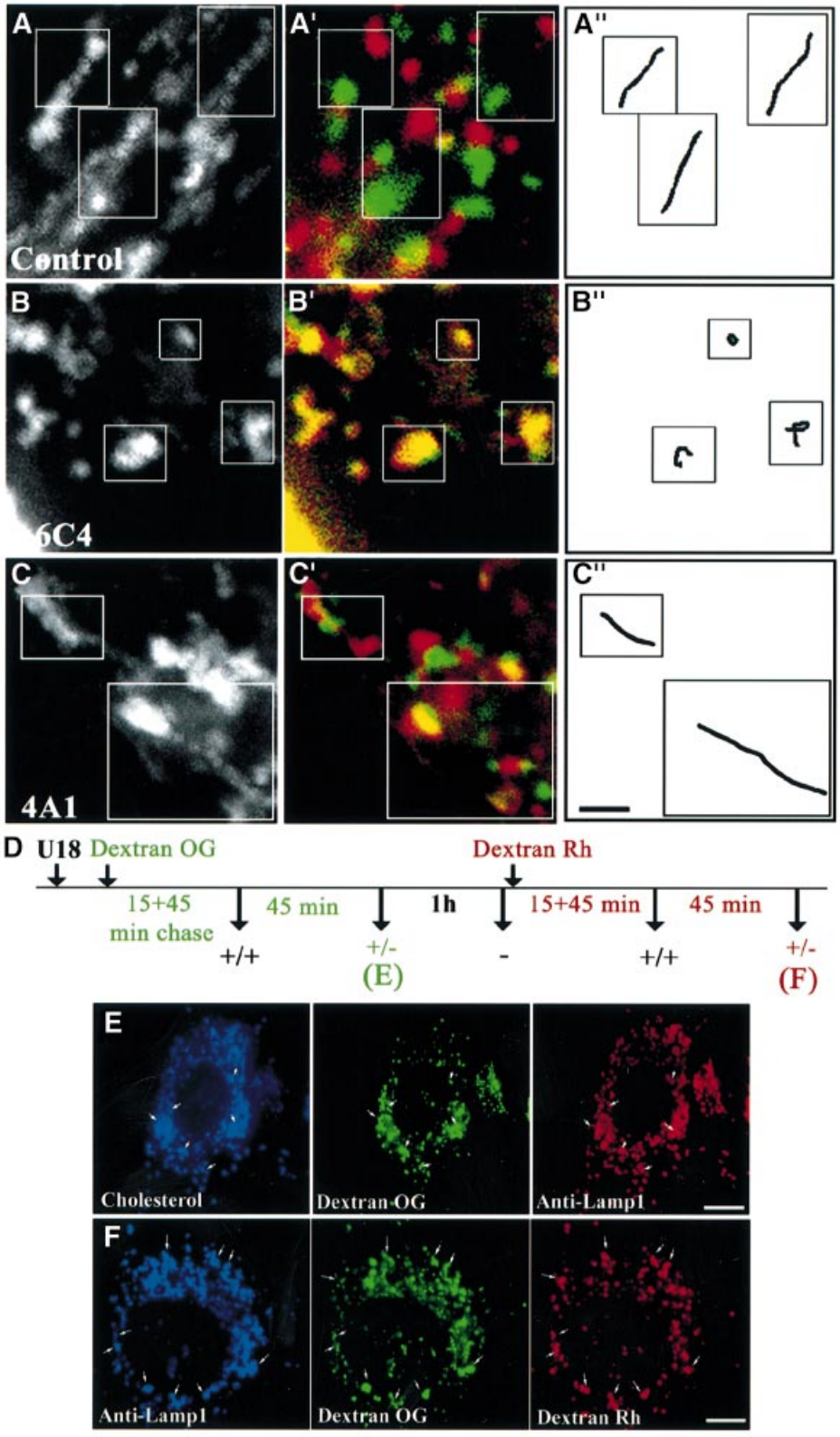

Fig. 3. Antibodies against LBPA and pulse–chase. (**A** and **B**) HeLa or (**C**) BHK cells transfected with CD63–GFP were incubated for 24 h without (A) or with the monoclonal antibody against LBPA (B; 6C4) or Lamp1 (C; 4A1). (We used BHK cells because large amounts of 4A1 were available; cholesterol also accumulates in BHK cells after 6C4 treatment; Kobayashi *et al*., 1999.) Motility was analyzed as in Figure 1. (**D**) Outline. HeLa cells treated for 10 h with U18666A (the drug remained present throughout the experiment), were labeled with a 15 min pulse of endocytosed Oregon green–dextran (Dextran OG). After a 45 min chase, labeled endosomes were clearly motile (+/+). Motility was low after a second 45 min chase (+/–) and abolished after a third 1 h chase (–). Then, cells were labeled with a second pulse of rhodamine–dextran (Dextran Rh), and the chase protocol was repeated. Samples were fixed and analyzed by triple-channel fluorescence microscopy after the first (**E**) and second (**F**) wave. Bars: (A–C) 1.5 μm; (E) 4 μm; (F) 2.4 μm.

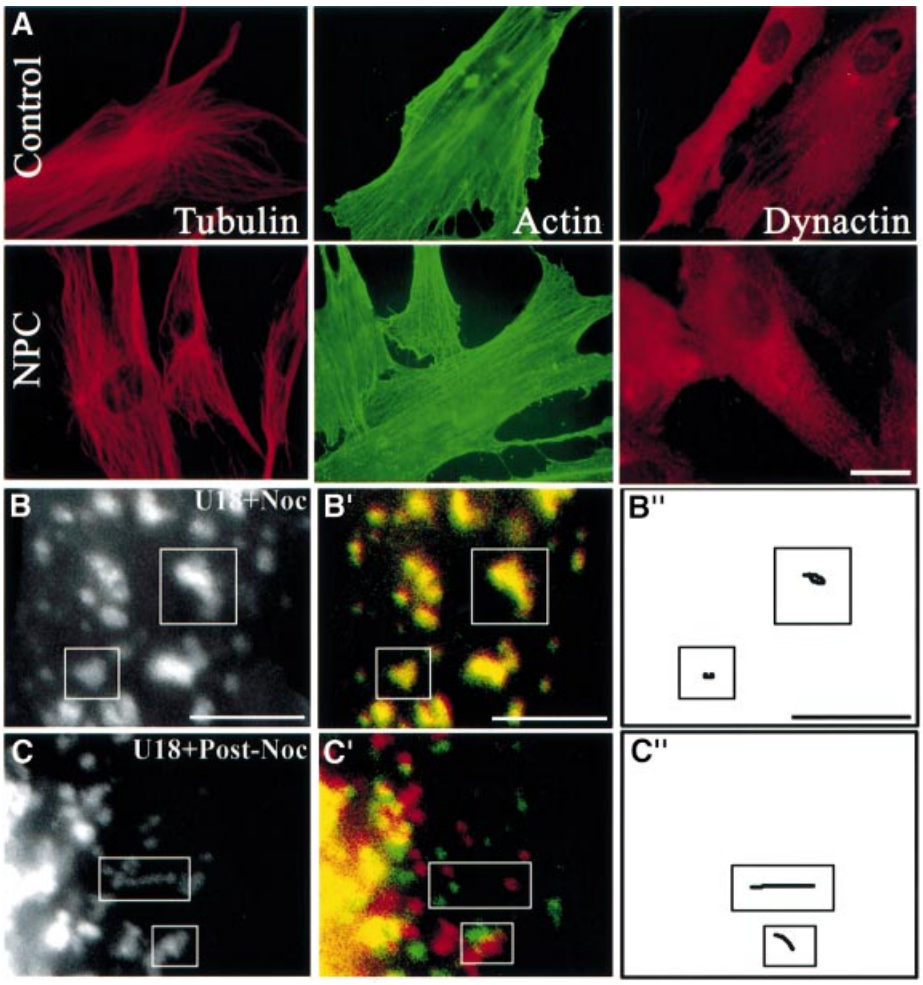

Fig. 4. Microtubules. (**A**) Control or NPC fibroblasts were labeled with the indicated antibodies. (**B** and **C**) HeLa cells transfected with CD63–GFP were treated for 13 h with U18666A, and the drug remained present throughout the experiment. Cells were then treated for 1 h with nocodazole (B; U18 + Noc) and then re-incubated for 90 min without nocodazole (C; U18 + Post-Noc). Motility analysis was as in Figure 1. Bars: (A) 8 μm; (B and C) 4 μm.

motility, since the same observations could be repeated with a second wave of rhodamine–dextran internalized into the same cells with the same pulse–chase protocol. At the end of the experiment, a significant portion of rhodamine– (second wave) and Oregon green–dextran (first wave) co-localized within immobile and swollen vesicles containing Lamp1 (Figure 3F), while Lamp1-positive compartments are normally highly motile (see above, not shown). Cholesterol accumulation thus selectively impaired motility, but not fusion.

Interactions with microtubules

Since motility depends on microtubules, we investigated whether inhibition was due to cytoskeletal alterations. However, similar amounts of the dynein activator dynactin (Vallee and Sheetz, 1996) were found on late endosomes of control or U18666A-treated cells after fractionation (not shown), and no difference was observed in the distribution of tubulin or dynactin when comparing NPC cells (Figure 4A) or U18666A-treated cells (not shown) with control cells. Neither was actin affected (Figure 4A), nor ezrin, a protein of the cortical actin cytoskeleton (Mangeat *et al*., 1999), CLIP170, a protein that may link endocytic vesicles to microtubules (Pierre *et al*., 1992), kinesin nor the APC-associated protein EB1 that interacts with components of the dynactin complex and with cytoplasmic dynein intermediate chain (Berrueta *et al*., 1999) (not shown). We then reasoned that microtubule binding might be impaired after cholesterol accumulation, since vesicles exhibited Brownian-type motion. Using a well-established sedimentation assay (Van der Sluijs *et al*., 1990; Pierre *et al*., 1992), we found that the capacity of late endocytic membranes prepared from U18666A-treated cells to bind taxol-polymerized microtubules was not impaired (not shown). Direct evidence for the interactions of cholesterol-laden vesicles with microtubules was obtained after their depolymerization with nocodazole. Not only were cholesterol-laden vesicles redistributed in the cytoplasm, much like in control cells, but motility was restored after nocodazole washout until vesicles eventually re-clustered in the perinuclear region, presumably via cytoplasmic dynein (Figure 4B and C). Thus, swollen, cholesterol-laden vesicles could not only bind microtubules, but also move after microtubule re-polymerization.

Motors and paralysis

Despite motility inhibition, it seemed likely that cytoplasmic dynein could interact with late endocytic vesicles

loaded with cholesterol, since these were clustered in the perinuclear region (Figure 2), and, even more strikingly, re-clustered in this region after nocodazole washout (Figure 4C). We found that motility could be partially restored in U18666A-treated cells after inhibition of cytoplasmic dynein by dynamitin overexpression (Figure 5B and E, U18 + dynamitin 1, compare with Figure 5A). Clearly, the motility of these large, swollen vesicles was somewhat sluggish when compared with highly dynamic vesicles and tubules in control cells. Consistently with the inhibition of minus-end-directed motility, movements appeared to be directed preferentially towards the periphery, presumably via kinesin. Indeed, motility was inhibited when scoring only peripheral vesicles (Figure 5B and E, U18 + dynamitin 2). These observations show that cytoplasmic dynein mediated

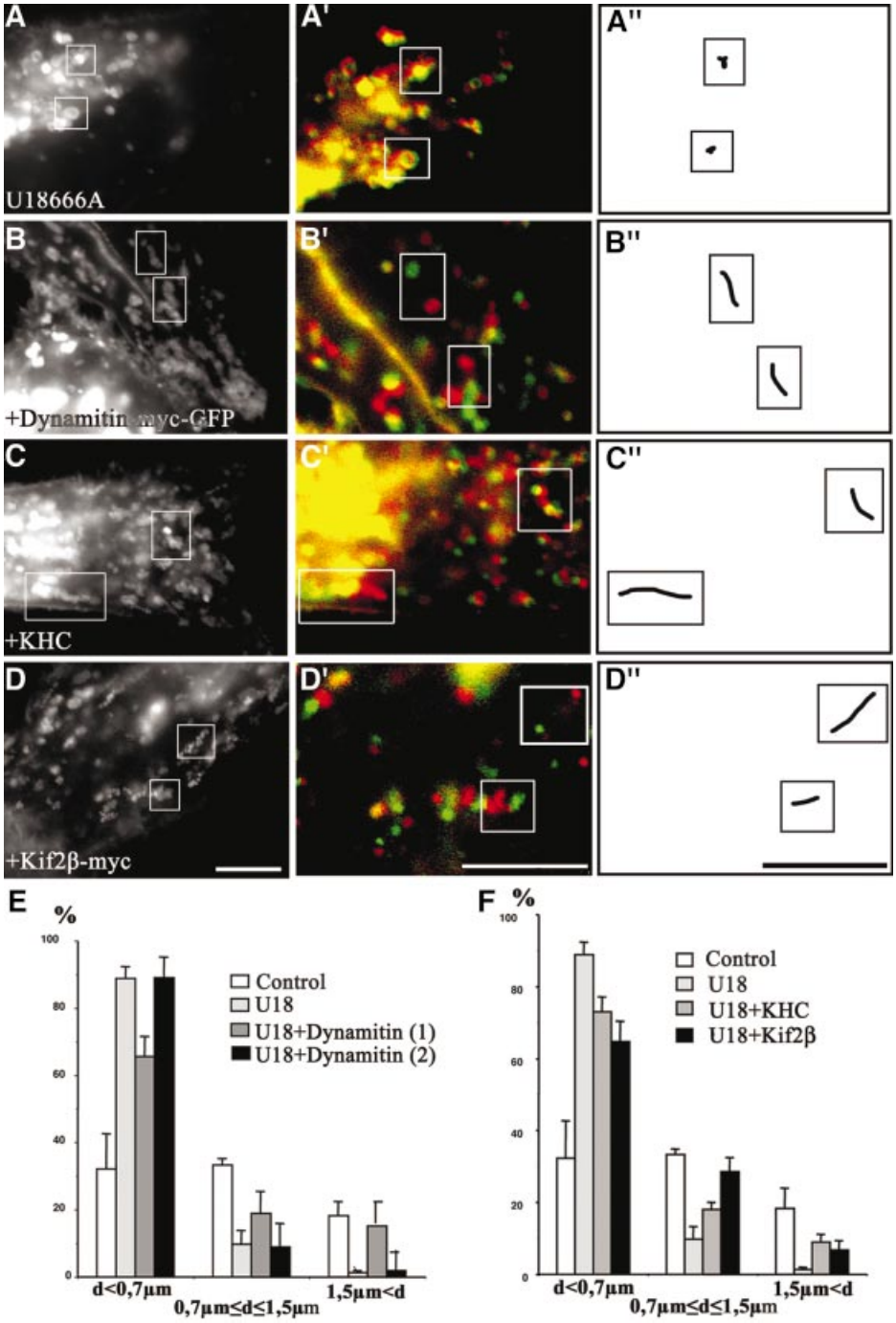

Fig. 5. Motors. Cells were transfected with CD63–GFP alone (**A**), or co-transfected with CD63–GFP and either dynamitin-myc–GFP (**B**), KHC (**C**) or Kif2β-myc (**D**). (As in Figure 1, overexpressed dynamitin remained cytosolic; co-expression was verified in all cases.) Cells were then treated with U18666A for 13 h. Motility analysis was as in Figure 1. Bars: 4 µm. (**E** and **F**) The bird's eye distances (not the trajectory) between initial and final positions were quantified after 25 s. Control, control without U18666A; U18, U18666A as in (A); U18 + Dynamitin, dynamitin and U18666A; motility was partially restored as in (B) (1), but stopped at the cell periphery (2); U18 + KHC, KHC and U18666A as in (C); U18 +Kif2β, Kif2β and U18666A as in (D).

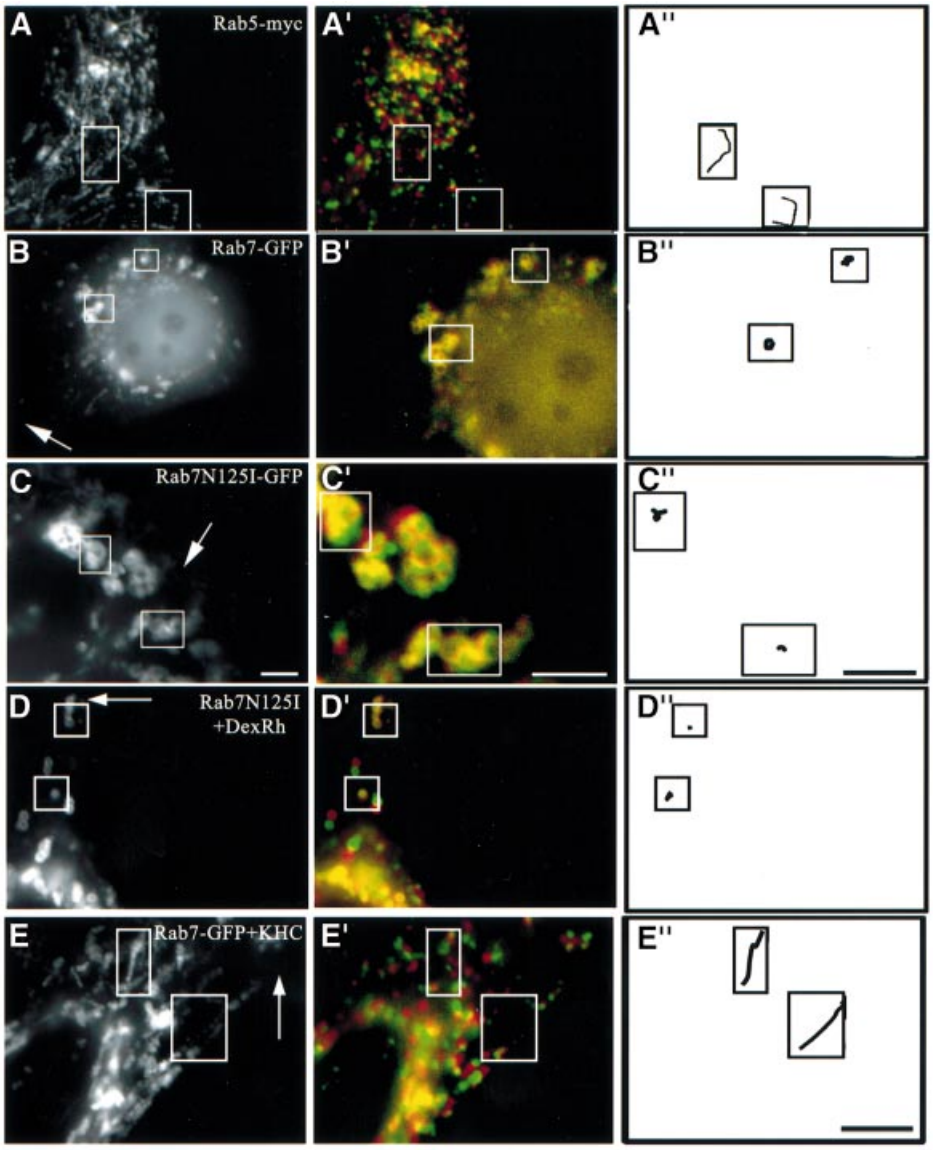

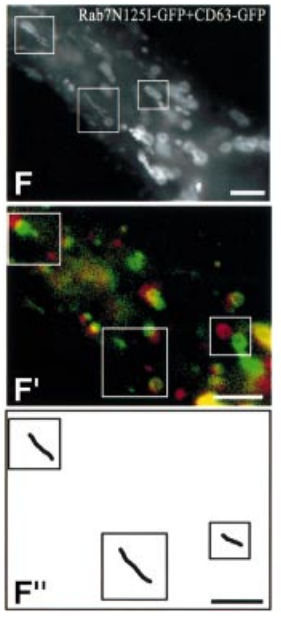

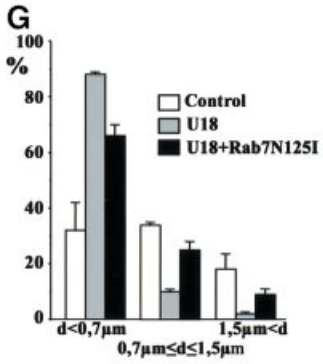

Fig. 6. Rab7 and cholesterol. (**A**) Co-transfection with CD63–GFP and Rab5-myc (co-expression was verified by immunofluorescence using anti-myc antibodies). (**B**) Transfection with Rab7–GFP. (**C**) Co-transfection with CD63–GFP and Rab7N125I–GFP (Rab7N125I–GFP remained cytosolic and was not detected after 100–200 ms exposure; co-expression was verified after longer exposures). (**D**) After transfection with Rab7N125I–GFP, late endocytic vesicles were labeled with a 15 min pulse of rhodamine–dextran (DexRh) followed by a 45 min chase, as in Figure 3D, to reveal better the partial redistribution to the periphery. (**E**) Cells co-transfected with Rab7–GFP and KHC were treated with U18666A for 13 h. (**F** and **G**) Cells co-transfected with CD63–GFP and Rab7N125I–GFP were treated with U18666A for 13 h (F), and distances between initial and final positions were quantified (G) as in Figure 5. Motility analysis was as in Figure 1. Arrows point to the cell periphery. Bars: (A, D and E) 4 µm; (B and C) 2 µm; (F) 2.8 µm.

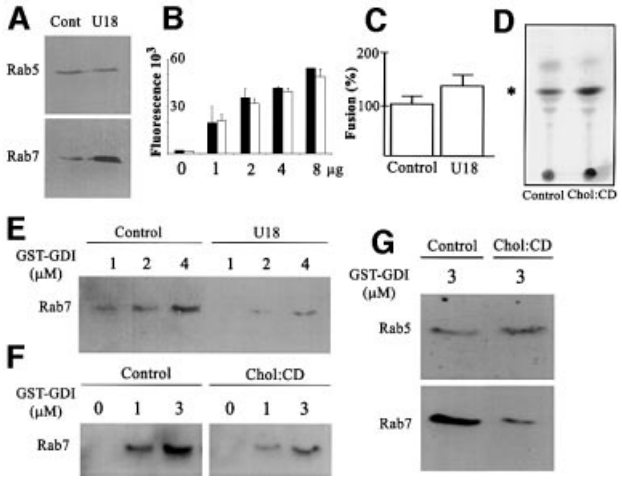

Fig. 7. Extraction by GDI. (**A** and **B**) Since fractionation properties can be altered by cholesterol accumulation (Lange *et al*., 1998), we prepared crude fractions containing both early and late endosomes from control (cont) or U18666A-treated (U18) BHK cells, so that samples and Rab protein content could be compared directly in the same experiment. Fractions were analyzed by western blotting with antibodies against Rab5 or Rab7 (A) or by ELISA using the anti-LBPA antibody (B; increasing amounts of fractions). (**C**) Homotypic fusion of late endosomes from control or U18666A-treated BHK cells. Fusion activity was normalized to the control. (**D**) Crude fractions from control cells were loaded (chol:CD) or not (control) with cholesterol *in vitro* using 1 mM cholesterol complexed to methyl-β-cyclodextrin. After flotation on gradients, membranes were collected, and lipids analyzed by TLC; the position of cholesterol is indicated. (**E**) Cells were treated (U18) or not (control) with U18666A. Crude fractions were incubated with 1, 2 or 4 µM GST–GDI (Cavalli *et al*., 2001). [To avoid any bias, control (~30 µg) and cholesterol-loaded membranes (~15 µg) were normalized to Rab7 itself.] Endosomes were removed by flotation in gradients. GST–GDI with captured Rab7 was recovered onto glutathione beads. Beads were analyzed by western blotting with anti-Rab7 antibodies. (**F**) Membranes loaded or not with cholesterol *in vitro* as in (D) were analyzed as in (E). (**G**) As (F), except that 3 µM GST–GDI was used, and analysis was with antibodies against Rab5 or Rab7.

cholesterol-laden vesicle motility towards the perinuclear region, hence that this minus-end-directed motor could still interact with and drive vesicles loaded with cholesterol.

Figure 5B also suggested that vesicles potentially could interact with kinesin, since plus-end-directed motility was restored after cytoplasmic dynein inactivation. Indeed, mild cytoplasm acidification, which stimulates kinesin activity (Verhey *et al*., 1998), partially restored the motility of swollen vesicles, eventually leading to their peripheral redistribution (not shown). Moreover, motility could be partially restored by overexpression of the ubiquitous conventional kinesin heavy chain HsuKHC/Kif5B (Figure 5C and F, compare with Figure 5A). Since kinesin light chains play a role in heavy chain motor activity or targeting (Verhey *et al*., 1998; Rahman *et al*., 1999), it is likely that excess KHC was associated with endogenous light chains. In addition, overexpression of Kif2β, which also supports late endocytic vesicle movement (Santama *et al*., 1998), also partially restored motility (Figure 5D and F), like KHC. After KHC or Kif2β overexpression, motility was bidirectional, presumably because both plus- and minus-end-directed motors could then act on endocytic membranes. These experiments clearly show that swollen vesicles loaded with cholesterol had not altogether lost the capacity to interact with kinesin. However, the data also show that vesicles could only use kinesin if cytoplasmic dynein was inhibited, or if kinesin was activated (after cytoplasm acidification) or overexpressed. Altogether, our observations show that, upon cholesterol loading, late endocytic vesicles are translocated to the perinuclear region by cytoplasmic dynein, where they remain, being unable to use kinesin and to move centripetally—a situation that eventually leads to paralysis.

The small GTPase Rab7

Evidence is accumulating that some small GTPases of the Rab family coordinate different mechanisms regulating traffic via several effectors, including interactions with microtubules (Chavrier and Goud, 1999; Zerial and McBride, 2001). Rab7 plays a crucial role in late endocytic traffic (Chavrier *et al*., 1990; Feng *et al*., 1995; Meresse *et al*., 1995; Mukhopadhyay *et al*., 1997; Papini *et al*., 1997; Vitelli *et al*., 1997; Bucci *et al*., 2000; Cantalupo *et al*., 2001), and recent studies show that the Rab7 effector RILP (Cantalupo *et al*., 2001) induces the recruitment of dynein–dynactin motors and regulates transport toward the minus-end of microtubules (Jordens *et al*., 2001). We first investigated whether Rab7 was involved in the dynamics of late endocytic networks. Overexpressed wild-type Rab7 was largely membrane associated, and co-localized with LBPA on late endosomes (not shown), like endogenous Rab7 (Kobayashi *et al*., 1998b). Then, late endocytic vesicles accumulated in the perinuclear region, as previously observed (Bucci *et al*., 2000), and motility was inhibited, except for Brownian-type motion (Figure 6B). The effects of Rab7 overexpression were specific, since overexpression of the early endosomal GTPase Rab5 had no effects on the motility of the late endocytic compartment (Figure 6A). Much like after cholesterol accumulation, it is likely that wild-type Rab7 overexpression caused endosome accumulation in the perinuclear region by increasing minus-end-directed motility (Cantalupo *et al*., 2001; Jordens *et al*., 2001), and thus reducing bi-directional motility, eventually leading to paralysis. Indeed, motility in cells overexpressing Rab7 could be partially restored by KHC co-overexpression (not shown; see Figure 6E). Conversely, overexpression of the Rab7 inhibitory mutant N125I also reduced motility (Figure 6C), but induced a partial redistribution of late endocytic compartments to the cell periphery (Figure 6D), as observed by Bucci *et al*. (2000). Altogether these data show that late endosome motility is regulated selectively by Rab7.

Next, we tested whether Rab7 was involved in motility inhibition after cholesterol accumulation, since the effects of cholesterol accumulation and Rab7 overexpression in control cells were pretty much identical. One may reason that if both Rab7 and cholesterol interfered with plus-end-directed motility through the same pathway, then motility should be partially restored after KHC overexpression. Indeed, Figure 6E shows that KHC overexpression could partially overcome the inhibitory effects of both wild-type Rab7 overexpression and cholesterol accumulation. Direct evidence for the role of Rab7 came from the observations that the motility of large and swollen vesicles in cells

treated with U18666A could be partially restored by the inhibitory mutant Rab7N125I (Figure 6F and G). Cholesterol accumulation still occurred, showing that Rab7 did not play a direct role in the biogenesis of cholesterol-laden vesicles. Obviously, overexpression of wild-type Rab7 or RILP did not restore motility (not shown), since wild-type Rab7 (Figure 6B) and RILP (Jordens *et al*., 2001) were already inhibitory without cholesterol accumulation. These observations thus indicate that Rab7 is part of the mechanism that regulates the capacity of late endocytic membranes loaded with cholesterol to switch from cytoplasmic dynein to kinesin.

Cholesterol accumulation interferes selectively with Rab7 extraction by GDI

Like other Rab proteins, Rab7 is tightly associated with the bilayer via geranylgeranylation of cysteine residues (Novick and Zerial, 1997; Zerial and McBride, 2001). Despite this modification, Rab proteins cycle between the membrane and cytosol, and this cycle depends on the guanine nucleotide dissociation inhibitor (GDI), which extracts Rab proteins bound to GDP from membranes and protects them in the cytosol (Sasaki *et al*., 1990; Cavalli *et al*., 2001). At steady state, roughly equal amounts of Rab7 are found on membranes and complexed to GDI in the cytosol (not shown). Since cholesterol is well known to alter membrane biophysical properties, and to reduce bilayer fluidity, its accumulation may well interfere with the Rab7 membrane–cytosol cycle. Strikingly, membrane-associated Rab7, but not Rab5, was increased after cholesterol accumulation (Figure 7A), with a concomitant decrease in cytosolic amounts (not shown). The amounts of late endocytic membranes analyzed in these experiments were identical with or without cholesterol accumulation, as judged from their LBPA content (Figure 7B). [The total cellular amounts of LBPA and Rab7 were not changed after U18666A treatment (not shown).] It is also well established that cholesterol accumulation decreases the fusion capacity of the bilayer. However, fusion was not inhibited by cholesterol accumulation (Figure 7C) in our well-established assay measuring late endosome fusion (Bomsel *et al*., 1990; Aniento *et al*., 1993), in agreement with light microscopy observations (Figure 3F). In fact, fusion was even stimulated (+38%), when compared with controls, and this increase was specific, since early endosome fusion was not affected under the same conditions (N.Mayran and J.Gruenberg, unpublished observations). Fusion activity presumably was retained despite cholesterol accumulation because of increased levels of membrane-associated Rab7, in agreement with its proposed role in late endosome fusion (Papini *et al*., 1997).

We then tested whether cholesterol accumulation directly interfered with extraction of membrane-associated Rab7 by GDI, perhaps because of the altered fluidity of the bilayer. Figure 7E shows that Rab7 was poorly extracted by GDI from membranes that had accumulated cholesterol *in vivo*, when compared with controls. To rule out some indirect effect of cholesterol accumulation *in vivo*, membranes were prepared from control cells and then loaded with cholesterol *in vitro*. When using 1 mM cholesterol complexed to methyl-β-cyclodextrin as donor (to prevent membrane overload), the membrane cholesterol content was increased ~2.5-fold (Figure 7D), and Rab7 extraction by GDI was inhibited to the same extent (Figure 7F) as after cholesterol accumulation *in vivo* (Figure 7E). Moreover, the effects were selective, since extraction of Rab5, which is present on early endosomes (Zerial and McBride, 2001), was not affected by cholesterol loading *in vivo* (Figure 7A) or *in vitro* (Figure 7G).

Discussion

We find that late endocytic compartments are paralyzed after cholesterol accumulation, including in fibroblasts from NPC patients, in agreement with recent observations (Ko *et al*., 2001; Zhang *et al*., 2001). Clearly, one may expect that reduced endosome motility contributes to the complex clinical picture of NPC, including perhaps sorting/trafficking defects (Kobayashi *et al*., 1999, 2000). The precise function of NPC1 is not known, perhaps pump activity (Davies *et al*., 2000) or retrograde transport of lysosomal cargo (Neufeld *et al*., 1999). One might also envisage that NPC1 is directly involved in motility control (Ko *et al*., 2001). However, our experiments with antibodies against LBPA or U18666A suggest rather that motility inhibition is an indirect consequence of NPC1 mutation, and is caused by cholesterol accumulation. In addition, we find that motility is not affected in Tay–Sachs fibroblasts, which do not accumulate cholesterol, indicating that all storage disorders are not accompanied by a motility defect. However, cholesterol accumulation occurs in a number of other sphingolipidoses (Chen *et al*., 1999; Puri *et al*., 1999). Whether motility is also impaired in these diseases remains to be determined.

Our data indicate that late endocytic compartments retain cytoplasmic dynein activity after cholesterol accumulation, but are unable to acquire kinesin activity. The simplest interpretation is that cholesterol loading interferes with the capacity of these organelles to switch from minus- to plus-end-directed motility, eventually resulting in a loss of bi-directional motility and paralysis. The small GTPase Rab7 seems to play a crucial role in this process, since the inhibitory mutant Rab7N125I restores motility of cholesterol-laden vesicles. Conversely, excess wild-type Rab7 inhibits motility in control cells. If the precise mechanism controlling this switch function, perhaps involving the Rab7 effector RILP (Cantalupo *et al*., 2001; Jordens *et al*., 2001), remains to be worked out, our data already indicate that membrane lipids are involved. Cholesterol accumulation increases the levels of Rab7 on membranes, with a concomitant decrease in the capacity of GDI to extract membrane-associated Rab7, presumably because changes in the bilayer fluidity render the Rab7 prenyl anchor less accessible to GDI. It is also possible that cholesterol directly interferes with Rab7 nucleotide exchange or hydrolysis capacity. In any case, cholesterol accumulation in late endocytic compartments affects the Rab7 cycle selectively, since Rab5 is not altered. This difference may be due to differences in the prenylation sites (Chavrier *et al*., 1991) or in the target membrane composition. Indeed, early, but not late, endosomes contain significant amounts of cholesterol (Kobayashi *et al*., 1998a), and Rab5, in contrast to Rab7, is predominantly membrane associated (Cavalli *et al*., 2001). In fact, cholesterol depletion *in vitro* facilitates Rab5 release from endosomes

(not shown), perhaps suggesting that cholesterol plays a role in membrane association of other Rab proteins.

In summary, our observations indicate that the net movement of late endocytic elements depends on Rab7, which in turn depends on the lipid composition. By controlling levels of membrane-associated Rab7 via GDI, changes in the membrane cholesterol content may thus modulate motor activity. To our knowledge, this is the first demonstration that motility can be regulated by the membrane lipid composition via the cycle of a Rab GTPase.

Materials and methods

Cells, antibodies and reagents

HeLa and BHK cells were grown as described (Gruenberg *et al*., 1989; Rojo *et al*., 1997), as well as cultured skin NPC or Tay–Sachs fibroblasts (Omura *et al*., 1989). NPC and Tay–Sachs fibroblasts were from H.Sakuraba (Tokyo Metropolitan Institute of Medical Sciences, Tokyo, Japan), and HeLa cells expressing NAGT1–GFP from G.Warren (Yale University, USA). Sources of antibodies were: monoclonal anti-CD63 antibodies: 2C6, U.Vischer (CMU, Geneva, Switzerland); 1B5, M.Marsh (UCL, London, UK); H5C6, J.Salamero (Institut Curie, Paris, France); antisera: human Lamp1, S.Carlsson (Umea University, Sweden); calnexin, A.Helenius (ETH, Zurich, Switzerland); polyclonal antibodies: cathepsin D, B.Hoflack (MPI, Dresden, Germany); giantin, M.Renz (University of Karlsruhe, Germany); antibodies against ezrin, P.Mangeat (University of Montpellier, France); and Suk4 antibody against kinesin, J.M.Scholey (UC Davis, CA). Monoclonal antibodies were purchased from: human Lamp1 (107a), Pharmingen (San Diego, CA); Lamp2 (H4B4), Developmental Studies Hybridoma Bank (Iowa City, IA), transferrin receptor, Boehringer Mannheim (Indianapolis, IN); α- and β-tubulin and dynactin, Sigma (Saint Louis, MO). Antibodies against dynactin and EB1 were from Transduction Laboratories (Laagstraat, Belgium); monoclonal and polyclonal antibodies against GFP from Clontech (Palo Alto, USA); polyclonal anti-myc antibodies from Santa Cruz Biotechnology (Santa Cruz, CA); and labeled secondary antibodies from Jackson ImmunoResearch Laboratories (West Grove, PA). Rhodamine–transferrin, Oregon green– and rhodamine–dextran were from Molecular Probes (Eugene, OR), U18666A from Biomol Research Laboratories (Plymouth Meeting, PA), and taxol and nocodazole from Sigma. Oregon green and Alexa 568 labeling of antibodies was according to the manufacture's instructions (Molecular Probes).

Plasmids

The plasmid containing CD63–GFP was obtained after cloning CD63 into a modified pEGFP-C1 (Clontech, Palo Alto, USA) vector with the CMV promoter replaced by the bos promoter (from G.Griffiths, School of Pathology, Oxford, UK). The plasmid containing Rab5-myc was obtained after cloning pGEM-1-Rab5 (from H.Stenmark, Oslo, Norway) into a pcDNA3 vector (from R.Regazzi, University of Lausanne, Switzerland). GFP–Rab7, GFP–Rab7N125I and GFP–lgp120/Lamp1 cDNAs were obtained from P.Boquet (INSERM452, Nice, France); RILP, conventional kinesin (KHC) and motor head-deleted mutant cDNAs from J.Neefjes (Netherlands Cancer Institute, Amsterdam, The Netherlands); myc-tagged Kif2β kinesin cDNA from N.Santama (University of Cyprus, Nicosia, Cyprus); and myc-tagged GFP–dynamitin cDNA from T.Schroer (Johns Hopkins University, Baltimore, MD). pECFP-mito encoding a fusion of ECFP to the targeting sequence of cytochrome *c* oxidase subunit VII was from Clontech.

In vivo analysis, microscopy and video microscopy

Cells were grown in chambered coverglasses (MatTeck Corporation, Ashland, MA), transfected 24 h after passage, and analyzed 36 h later. Endogenous CD63 was labeled as described (Kobayashi *et al*., 2000). In some cases, cells were incubated with 2.5 mg/ml Oregon green- or rhodamine-labeled dextran for 15 min at 37°C, washed and re-incubated without marker as indicated. When indicated, cells were pre-incubated for 5–15 h at 37°C with 3 μg/ml U18666A or for 24 h with ~100 μg/ml monoclonal antibody against LBPA (6C4) or BHK Lamp1 (4A1) (Kobayashi *et al*., 1999, 2000). Microtubules or actin filaments were depolymerized using 1 μM nocodazole for 2 h, or 10^{-5} M cytochalasin D for 1 h, respectively. When indicated, cells were treated with 20 μg/ml brefeldin A for 60 min at 37°C. For video microscopy, we used a Zeiss Axiovert S1000TV fluorescence microscope, a 50 W Hg lamp attenuated by transmission neutral-density filters (Omega Optical, Brattleboro, VT), a CCD camera C4742-95-12NRB (Hamamatsu-City, Japan) and OpenLab Software (Improvision, Coventry, UK); exposure time: 100–200 ms. Temperature (37°C) and atmosphere (5% CO_2) control was with the CTI-3700/37-2-Digital system (PeCon, Erbach-Bach, Germany). Pictures were processed in AdobePhotoshop 5.0 or converted into Quicktime movies using OpenLab. Traces and distances were measured manually. Quantification was always done on three separate experiments, and in each experiment motility was analyzed on all vesicles in three separate cells (~100 structures/cell, i.e. 900 per condition). Immunofluorescence microscopy and cholesterol staining with filipin were as described (Kobayashi *et al*., 1998b).

Biochemical methods

BHK early and late endosomal fractions (Aniento *et al*., 1993), rat liver cytosol (Aniento *et al*., 1993), HeLa cytosol (Cavalli *et al*., 2001) and crude fractions containing both early and late endosomes (Huber *et al*., 2000) were prepared as described. Homotypic fusion of late endosomes was measured using an established assay (Bomsel *et al*., 1990; Aniento *et al*., 1993). *In vitro* capture of Rab7 by GDI was as described (Cavalli *et al*., 2001), except that fractions containing both early and late endosomes were used. Cholesterol was loaded *in vitro* using cholesterol:methyl-β-cyclodextrin (Thiele *et al*., 2000), and membranes were retrieved to remove excess cholesterol (Cavalli *et al*., 2001). Thin-layer chromatography (Kobayashi *et al*., 1998b) and LBPA quantification by enzyme-linked immunosorbent assay (Kobayashi *et al*., 1998b) were as described.

Supplementary data

Supplementary data for this paper are available at *The EMBO Journal* Online.

Acknowledgements

We are particularly grateful to Marie-Hélène Beuchat, Bernard Schwendimann and Monique Beulet for expert technical assistance. We also wish to thank Gisou Van der Goot, Karl Matter and Jean-Claude Martinou for critical reading of the manuscript. C.L. was a recipient of a fellowship from the French Cancer Research Foundation. This work was supported by grants nos 31-37296.93 and 31/55325.98 from the Swiss National Science Foundation and by grant RG0260/19999-M from the International Human Frontier Science Program (to J.G.).

References

Allan,V.J. and Schroer,T.A. (1999) Membrane motors. *Curr. Opin. Cell Biol.*, **11**, 476–482.

Aniento,F., Emans,N., Griffiths,G. and Gruenberg,J. (1993) Cytoplasmic dynein-dependent vesicular transport from early to late endosomes [published erratum appears in *J. Cell Biol*. (1994) **124**, 397]. *J. Cell Biol.*, **123**, 1373–1387.

Berrueta,L., Tirnauer,J.S., Schuyler,S.C., Pellman,D. and Bierer,B.E. (1999) The APC-associated protein EB1 associates with components of the dynactin complex and cytoplasmic dynein intermediate chain. *Curr. Biol.*, **9**, 425–428.

Bomsel,M., Parton,R., Kuznetsov,S.A., Schroer,T.A. and Gruenberg,J. (1990) Microtubule and motor dependent fusion *in vitro* between apical and basolateral endocytic vesicles from MDCK cells. *Cell*, **62**, 719–731.

Bucci,C., Thomsen,P., Nicoziani,P., McCarthy,J. and van Deurs,B. (2000) Rab7: a key to lysosome biogenesis. *Mol. Biol. Cell.*, **11**, 467–480.

Cantalupo,G., Alifano,P., Roberti,V., Bruni,C.B. and Bucci,C. (2001) Rab-interacting lysosomal protein (RILP): the Rab7 effector required for transport to lysosomes. *EMBO J.*, **20**, 683–693.

Cavalli,V., Vilbois,F., Corti,M., Marcote,M.J., Tamura,K., Karin,M., Arkinstall,S. and Gruenberg,J. (2001) The stress-induced MAP kinase p38 regulates endocytic trafficking via the GDI:Rab5 complex. *Mol. Cell*, **7**, 421–432.

Chavrier,P. and Goud,B. (1999) The role of ARF and Rab GTPases in membrane transport. *Curr. Opin. Cell Biol.*, **11**, 466–475.

Chavrier,P., Parton,R.G., Hauri,H.P., Simons,K. and Zerial,M. (1990)

Localization of low molecular weight GTP binding proteins to exocytic and endocytic compartments. *Cell*, **62**, 317–329.
Chavrier,P., Gorvel,J.P., Stelzer,E., Simons,K., Gruenberg,J. and Zerial,M. (1991) Hypervariable C-terminal domain of rab proteins acts as a targeting signal. *Nature*, **353**, 769–772.
Chen,C.-S., Patterson,M.C., Wheatley,C.L., O'Brien,J.F. and Pagano,R.E. (1999) Broad screening test for sphingolipid-storage diseases. *Lancet*, **354**, 901–905.
Davies,J.P., Chen,F.W. and Ioannou,Y.A. (2000) Transmembrane molecular pump activity of Niemann–Pick C1 protein. *Science*, **290**, 2295–2298.
Escola,J.M., Kleijmeer,M.J., Stoorvogel,W., Griffith,J.M., Yoshie,O. and Geuze,H.J. (1998) Selective enrichment of tetraspan proteins on the internal vesicles of multivesicular endosomes and on exosomes secreted by human B-lymphocytes. *J. Biol. Chem.*, **273**, 20121–20127.
Feiguin,F., Ferreira,A., Kosik,K.S. and Caceres,A. (1994) Kinesin-mediated organelle translocation revealed by specific cellular manipulations. *J. Cell Biol.*, **127**, 1021–1039.
Feng,Y., Press,B. and Wandinger,N.A. (1995) Rab 7: an important regulator of late endocytic membrane traffic. *J. Cell Biol.*, **131**, 1435–1452.
Fukuda,M. (1991) Lysosomal membrane glycoproteins. Structure, biosynthesis and intracellular trafficking. *J. Biol. Chem.*, **266**, 21327–21330.
Gillooly,D.J., Morrow,I.C., Lindsay,M., Gould,R., Bryant,N.J., Gaullier,J.M., Parton,R.G. and Stenmark,H. (2000) Localization of phosphatidylinositol 3-phosphate in yeast and mammalian cells. *EMBO J.*, **19**, 4577–4588.
Griffiths,G., Hoflack,B., Simons,K., Mellman,I. and Kornfeld,S. (1988) The mannose 6-phosphate receptor and the biogenesis of lysosomes. *Cell*, **52**, 329–341.
Gruenberg,J. (2001) The endocytic pathway: a mosaic of domains. *Nature Rev. Mol. Cell Biol.*, **2**, 721–730.
Gruenberg,J., Griffiths,G. and Howell,K.E. (1989) Characterization of the early endosome and putative endocytic carrier vesicles *in vivo* and with an assay of vesicle fusion *in vitro*. *J. Cell Biol.*, **108**, 1301–1316.
Harada,A., Takei,Y., Kanai,Y., Tanaka,Y., Nonaka,S. and Hirokawa,N. (1998) Golgi vesiculation and lysosome dispersion in cells lacking cytoplasmic dynein. *J. Cell Biol.*, **141**, 51–59.
Herman,B. and Albertini,D.F. (1984) A time-lapse video image intensification analysis of cytoplasmic organelle movements during endosome translocation. *J. Cell Biol.*, **98**, 565–576.
Hollenbeck,P.J. and Swanson,J.A. (1990) Radial extension of macrophage tubular lysosomes supported by kinesin. *Nature*, **346**, 864–866.
Huber,L., Fialka,I., Paiha,K., Hunzinker,W., Sacks,D.B., Bähler,M., Way,M., Gagescu,R. and Gruenberg,J. (2000) Both calmodulin and the unconventional myosin myr4 regulate membrane trafficking along the recycling pathway of MDCK cells. *Traffic*, **1**, 494–503.
Jordens,I., Fernandez-Borja,M., Marsman,M., Dusseljee,S., Janssen,L., Calafat,J., Janssen,H., Wubbolts,R. and Neefjes,J. (2001) The Rab7 effector protein RILP controls lysosomal transport by inducing the recruitment of dynein–dynactin motors. *Curr. Biol.*, **11**, 1680–1685.
Ko,D.C., Gordon,M.D., Jin,J.Y. and Scott,M.P. (2001) Dynamic movements of organelles containing Niemann–Pick C1 protein: NPC1 involvement in late endocytic events. *Mol. Biol. Cell*, **12**, 601–614.
Kobayashi,T., Gu,F. and Gruenberg,J. (1998a) Lipids and lipid domains in endocytic membrane traffic. *Semin. Cell Dev. Biol.*, **9**, 517–526.
Kobayashi,T., Stang,E., Fang,K.S., de,M.P., Parton,R.G. and Gruenberg,J. (1998b) A lipid associated with the antiphospholipid syndrome regulates endosome structure and function. *Nature*, **392**, 193–197.
Kobayashi,T., Beuchat,M.H., Lindsay,M., Frias,S., Palmiter,R.D., Sakuraba,H., Parton,R.G. and Gruenberg,J. (1999) Late endosomal membranes rich in lysobisphosphatidic acid regulate cholesterol transport. *Nature Cell Biol.*, **1**, 113–118.
Kobayashi,T., Vischer,U.M., Rosnoblet,C., Lebrand,C., Lindsay,M., Parton,R.G., Kruithof,E.K. and Gruenberg,J. (2000) The tetraspanin CD63/lamp3 cycles between endocytic and secretory compartments in human endothelial cells. *Mol. Biol. Cell*, **11**, 1829–1843.
Kornfeld,S. and Mellman,I. (1989) The biogenesis of lysosomes. *Annu. Rev. Cell. Biol.*, **5**, 483–526.
Lange,Y., Ye,J. and Steck,T.L. (1998) Circulation of cholesterol between lysosomes and the plasma membrane. *J. Biol. Chem.*, **273**, 18915–18922.
Lippincott-Schwartz,J., Donaldson,J.G., Schweizer,A., Berger,E.G., Hauri,H.P., Yuan,L.C. and Klausner,R.D. (1990) Microtubule-dependent retrograde transport of proteins into the ER in the presence of brefeldin A suggests an ER recycling pathway. *Cell*, **60**, 821–836.
Liscum,L. and Faust,J.R. (1989) The intracellular transport of low density lipoprotein-derived cholesterol is inhibited in Chinese hamster ovary cells cultured with 3-β-[2-(diethylamino)ethoxy]androst-5-en-17-one. *J. Biol. Chem.*, **264**, 11796–11806.
Liscum,L. and Klansek,J.J. (1998) Niemann–Pick disease type C. *Curr. Opin. Lipidol.*, **9**, 131–135.
Mangeat,P., Roy,C. and Martin,M. (1999) ERM proteins in cell adhesion and membrane dynamics. *Trends Cell Biol.*, **9**, 187–192.
Mayor,S., Sabharanjak,S. and Maxfield,F.R. (1998) Cholesterol-dependent retention of GPI-anchored proteins in endosomes. *EMBO J.*, **17**, 4626–4638.
Meresse,S., Gorvel,J.P. and Chavrier,P. (1995) The rab7 GTPase resides on a vesicular compartment connected to lysosomes. *J. Cell Sci.*, **108**, 3349–3358.
Metzelaar,M.J., Wijngaard,P.L., Peters,P.J., Sixma,J.J., Nieuwenhuis, H.K. and Clevers,H.C. (1991) CD63 antigen. A novel lysosomal membrane glycoprotein, cloned by a screening procedure for intracellular antigens in eukaryotic cells. *J. Biol. Chem.*, **266**, 3239–3245.
Mukhopadhyay,A., Funato,K. and Stahl,P.D. (1997) Rab7 regulates transport from early to late endocytic compartments in *Xenopus* oocytes. *J. Biol. Chem.*, **272**, 13055–13059.
Mullock,B.M., Bright,N.A., Fearon,C.W., Gray,S.R. and Luzio,J.P. (1998) Fusion of lysosomes with late endosomes produces a hybrid organelle of intermediate density and is NSF dependent. *J. Cell Biol.*, **140**, 591–601.
Neufeld,E.F. (1991) Lysosomal storage diseases. *Annu. Rev. Biochem.*, **60**, 257–280.
Neufeld,E.B. *et al*. (1999) The Niemann–Pick C1 protein resides in a vesicular compartment linked to retrograde transport of multiple lysosomal cargo. *J. Biol. Chem.*, **274**, 9627–9635.
Novick,P. and Zerial,M. (1997) The diversity of Rab proteins in vesicle transport. *Curr. Opin. Cell Biol.*, **9**, 496–504.
Oda,H., Stockert,R.J., Collins,C., Wang,H., Novikoff,P.M., Satir,P. and Wolkoff,A.W. (1995) Interaction of the microtubule cytoskeleton with endocytic vesicles and cytoplasmic dynein in cultured rat hepatocytes. *J. Biol. Chem.*, **270**, 15242–15249.
Omura,K., Suzuki,Y., Norose,N., Sato,M., Maruyama,K. and Koeda,T. (1989) Type C Niemann–Pick disease: clinical and biochemical studies on 6 cases. *Brain Dev.*, **11**, 57–61.
Papini,E., Satin,B., Bucci,C., de Bernard,M., Telford,J.L., Manetti,R., Rappuoli,R., Zerial,M. and Montecucco,C. (1997) The small GTP binding protein rab7 is essential for cellular vacuolation induced by *Helicobacter pylori* cytotoxin. *EMBO J.*, **16**, 15–24.
Pastan,I. and Willingham,W.C. (1981) Journey to the center of the cell: role of the receptosome. *Science*, **214**, 504–509.
Pierre,P., Scheel,J., Rickard,J.E. and Kreis,T.E. (1992) CLIP-170 links endocytic vesicles to microtubules. *Cell*, **70**, 887–900.
Puri,V., Watanabe,R., Dominguez,M., Sun,X., Wheatley,C.L., Marks, D.L. and Pagano,R.E. (1999) Cholesterol modulates membrane traffic along the endocytic pathway in sphingolipid-storage diseases. *Nature Cell Biol.*, **1**, 386–388.
Rahman,A., Kamal,A., Roberts,E.A. and Goldstein,L.S. (1999) Defective kinesin heavy chain behavior in mouse kinesin light chain mutants. *J. Cell Biol.*, **146**, 1277–1288.
Rodriguez,A., Samoff,E., Rioult,M.G., Chung,A. and Andrews,N.W. (1996) Host cell invasion by trypanosomes requires lysosomes and microtubule/kinesin-mediated transport. *J. Cell Biol.*, **134**, 349–362.
Rojo,M., Pepperkok,R., Emery,G., Kellner,R., Stang,E., Parton,R.G. and Gruenberg,J. (1997) Involvement of the transmembrane protein p23 in biosynthetic protein transport. *J. Cell Biol.*, **139**, 1119–1135.
Santama,N., Krijnse-Locker,J., Griffiths,G., Noda,Y., Hirokawa,N. and Dotti,C.G. (1998) KIF2β, a new kinesin superfamily protein in non-neuronal cells, is associated with lysosomes and may be implicated in their centrifugal translocation. *EMBO J.*, **17**, 5855–5867.
Sasaki,T., Kikuchi,A., Araki,S., Hata,Y., Isomura,M., Kuroda,S. and Takai,Y. (1990) Purification and characterization from bovine brain cytosol of a protein that inhibits the dissociation of GDP from and the subsequent binding of GTP to smg p25A, a ras p21-like GTP-binding protein. *J. Biol. Chem.*, **265**, 2333–2337.
Schroer,T.A. and Sheetz,M.P. (1991) Functions of microtubule-based motors. *Annu. Rev. Physiol.*, **53**, 629–652.
Shima,D.T., Haldar,K., Pepperkok,R., Watson,R. and Warren,G. (1997)

Partitioning of the Golgi apparatus during mitosis in living HeLa cells. *J. Cell Biol.*, **137**, 1211–1228.
Simonsen,A. and Stenmark,H. (2001) PX domains: attracted by phosphoinositides. *Nature Cell Biol.*, **3**, E179–E182.
Simonsen,A., Wurmser,A.E., Emr,S.D. and Stenmark,H. (2001) The role of phosphoinositides in membrane transport. *Curr. Opin. Cell Biol.*, **13**, 485–492.
Tanaka,Y., Kanai,Y., Okada,Y., Nonaka,S., Takeda,S., Harada,A. and Hirokawa,N. (1998) Targeted disruption of mouse conventional kinesin heavy chain, kif5B, results in abnormal perinuclear clustering of mitochondria. *Cell*, **93**, 1147–1158.
Thiele,C., Hannah,M.J., Fahrenholz,F. and Huttner,W.B. (2000) Cholesterol binds to synaptophysin and is required for biogenesis of synaptic vesicles. *Nature Cell Biol.*, **2**, 42–49.
Valetti,C., Wetzel,D.M., Schrader,M., Hasbani,M.J., Gill,S.R., Kreis,T.E. and Schroer,T.A. (1999) Role of dynactin in endocytic traffic: effects of dynamitin overexpression and colocalization with CLIP-170. *Mol. Biol. Cell*, **10**, 4107–4120.
Vallee,R.B. and Sheetz,M.P. (1996) Targeting of motor proteins. *Science*, **271**, 1539–1544.
Van der Sluijs,P., Bennett,M.K., Antony,C., Simons,K. and Kreis,T.E. (1990) Binding of exocytic vesicles from MDCK cells to microtubules *in vitro*. *J. Cell Sci.*, **95**, 545–553.
Verhey,K.J., Lizotte,D.L., Abramson,T., Barenboim,L., Schnapp,B.J. and Rapoport,T.A. (1998) Light chain-dependent regulation of kinesin's interaction with microtubules. *J. Cell Biol.*, **143**, 1053–1066.
Vitelli,R., Santillo,M., Lattero,D., Chiariello,M., Bifulco,M., Bruni,C.B. and Bucci,C. (1997) Role of the small GTPase Rab7 in the late endocytic pathway. *J. Biol. Chem.*, **272**, 4391–4397.
Wubbolts,R., Fernandez-Borja,M., Jordens,I., Reits,E., Dusseljee,S., Echeverri,C., Vallee,R.B. and Neefjes,J. (1999) Opposing motor activities of dynein and kinesin determine retention and transport of MHC class II-containing compartments. *J. Cell Sci.*, **112**, 785–795.
Zerial,M. and McBride,H. (2001) Rab proteins as membrane organizers. *Nature Rev. Mol. Cell Biol.*, **2**, 107–117.
Zhang,M., Dwyer,N.K., Love,D.C., Cooney,A., Comly,M., Neufeld,E., Pentchev,P.G., Blanchette-Mackie,E.J. and Hanover,J.A. (2001) Cessation of rapid late endosomal tubulovesicular trafficking in Niemann–Pick type C1 disease. *Proc. Natl Acad. Sci. USA*, **98**, 4466–4471.

Received September 4, 2001; revised January 14, 2002; accepted January 22, 2002